SYMMETRIC GAIN OPTOELECTRONIC MIXERS FOR LADAR

Stephen Drew, Nuri W. Emanetoglu*
Electrical and Computer Engineering Department, University of Maine
5708 Barrows Hall, Orono, ME 04469

Neal Bambha, Justin R. Bickford
US Army Research Laboratory, Sensors and Electron Devices Directorate
2800 Powder Mill Rd, Adelphi, MD, 20783

ABSTRACT

We are developing a symmetric gain optoelectronic mixer for chirped-AM laser detection and ranging systems (LADAR) operating in the "eye-safe" 1.55 μm wavelength range. Signal processing of a chirped-AM LADAR system is simplified if the photodetector in the receiver is used as an optoelectronic mixer (OEM). Adding gain to the optoelectronic mixer allows the following transimpedance amplifier's gain to be reduced, increasing bandwidth and improving the system's noise performance. The symmetric gain optoelectronic mixer is based on a symmetric heterojunction phototransistor. The base layer is $In_{0.53}Ga_{0.47}As$ (InGaAs), and the emitter/ collector layer is $In_{0.48}Al_{0.52}As$ (InAlAs). Two dimensional simulations of the devices were carried out to analyze device performance. Two sample heterostructures were grown using molecular beam epitaxy. We are currently in the prototype development stage. Simulation results and preliminary results from the initial batch of devices are presented. These symmetric gain optoelectronic mixer devices can lead to miniaturized LADAR-on-chip system. Such a system will have many military and civilian applications, such as range finding, terrain mapping, reconnaissance, and face recognition.

1. INTRODUCTION

The Army Research Laboratory (ARL) has been developing chirped-AM laser detection and ranging (LADAR) systems for applications such as reconnaissance, terrain mapping, force protection, facial recognition, robotic navigation and weapons fuzing. Signal processing of a chirped-AM LADAR system is simplified if the photodetector in the receiver is used as an optoelectronic mixer (OEM) [Ruff, *et al.* 2000]. A symmetric I-V characteristic photodetector can be used as an optoelectronic mixer. This allows driving the OEM directly with the local oscillator (LO) signal, without a DC bias. Sensitivity to background light is reduced, as the response from background light averages to zero. An additional 3 dB signal processing gain is also obtained. The OEM output is the low frequency difference signal, several orders of magnitude lower than the LO signal. Therefore, the gain of the transimpedance amplifier (TZA) following the photodetector can be increased, improving LADAR range. The metal-semiconductor-metal (MSM) Schottky detector is such a symmetric device. ARL has previously demonstrated chirped FM LADAR systems with GaAs and InGaAs MSM OEMs for operation at the 808 nm [Ruff, *et al.* 2000, Shen *et al.* 2002] and 1550 nm [Shen, *et al.* 2003, Shen *et al.* 2004] wavelengths.

A symmetric photodetector with gain would improve overall system performance, while preserving the advantages offered by MSM OEM devices. An OEM with gain would allow the gain of the following transimpedance amplifier to be reduced, increasing the TZA frequency bandwidth and improving overall system performance. Such a device can be based on the heterojunction phototransistor (HPT) or the modulated barrier diode (MBD), also known as a Camel diode.

The basic heterojunction photo transistor is a two terminal device, with the emitter made of a semiconductor which has a wider bandgap than the base and collector regions. A number of modifications to the basic HPT structure have been investigated to improve performance. A base bias can be provided, either optically or by an electrical contact [Chandrasekhar, *et al.* 1991]. The base composition can be graded to establish an electric field which enhances electron transport [Capasso, *et al.* 1983, Thuret, *et al.* 1999]. Improvements in material growth, device design and fabrication techniques have increased the maximum bandwidth of HPTs to the tens of GHz range [Choi, *et al.* 2005, Polleux, *et al.* 2004]. HPT responsivity typically increases with increasing optical power. This has been attributed to recombination at the base-emitter heterojunction. It is desirable to have gain independent from the optical power, or have larger gain at lower optical power levels. One approach to improve the gain dependence on optical power is to adjust the doping profile of the emitter and base layers of InP emitter/InGaAs base HPTs [Lue, *et al.* 1991]. By reducing the emitter doping in a thin layer at the emitter-base junction, the quantum well trapping of the electrons at this interface was reduced. The recombination currents were thus reduced, and the ideality factor of the transistor

Report Documentation Page

Form Approved
OMB No. 0704-0188

Public reporting burden for the collection of information is estimated to average 1 hour per response, including the time for reviewing instructions, searching existing data sources, gathering and maintaining the data needed, and completing and reviewing the collection of information. Send comments regarding this burden estimate or any other aspect of this collection of information, including suggestions for reducing this burden, to Washington Headquarters Services, Directorate for Information Operations and Reports, 1215 Jefferson Davis Highway, Suite 1204, Arlington VA 22202-4302. Respondents should be aware that notwithstanding any other provision of law, no person shall be subject to a penalty for failing to comply with a collection of information if it does not display a currently valid OMB control number.

1. REPORT DATE	2. REPORT TYPE	3. DATES COVERED
DEC 2008	**N/A**	**-**

4. TITLE AND SUBTITLE	5a. CONTRACT NUMBER
Symmetric Gain Optoelectronic Mixers For Ladar	5b. GRANT NUMBER
	5c. PROGRAM ELEMENT NUMBER
6. AUTHOR(S)	5d. PROJECT NUMBER
	5e. TASK NUMBER
	5f. WORK UNIT NUMBER
7. PERFORMING ORGANIZATION NAME(S) AND ADDRESS(ES)	8. PERFORMING ORGANIZATION REPORT NUMBER
Electrical and Computer Engineering Department, University of Maine 5708 Barrows Hall, Orono, ME 04469	
9. SPONSORING/MONITORING AGENCY NAME(S) AND ADDRESS(ES)	10. SPONSOR/MONITOR'S ACRONYM(S)
	11. SPONSOR/MONITOR'S REPORT NUMBER(S)

12. DISTRIBUTION/AVAILABILITY STATEMENT

Approved for public release, distribution unlimited

13. SUPPLEMENTARY NOTES

See also ADM002187. Proceedings of the Army Science Conference (26th) Held in Orlando, Florida on 1-4 December 2008, The original document contains color images.

14. ABSTRACT

15. SUBJECT TERMS

16. SECURITY CLASSIFICATION OF:			17. LIMITATION OF ABSTRACT	18. NUMBER OF PAGES	19a. NAME OF RESPONSIBLE PERSON
a. REPORT	b. ABSTRACT	c. THIS PAGE			
unclassified	**unclassified**	**unclassified**	**UU**	**6**	

improved, leading to a flattening of the gain vs. incident power characteristics. HPTs have been demonstrated for optoelectronic mixing applications, where the LO signal was provided electrically [Choi, *et al.* 2005, Liu, *et al.* 1997] or optically [Van de Casteele, *et al.*, 1996].

The modulated barrier diode, also known as the Camel diode, is a non-Schottky majority carrier diode in which the carrier transport is controlled by a potential barrier in the bulk of the semiconductor. The application of MBDs as photodetectors was first demonstrated by A.Y. Cho and co-workers [Chen, *et al.* 1981, Chen 1981]. The gain of the MBD is due to the hole trapping at the heterostructure interface. As holes accumulate in this quantum well, the barrier height will be lowered, resulting in an increased electron current, thus providing gain. As a majority carrier device, the MBD has fast intrinsic response [Chen, *et al.* 1981, Bethea, *et al.* 1982]. In contrast with the HPT, the MBD device has higher responsivity at lower optical power levels. The MBD has been used in a front-end photoreceiver, integrated with an FET [Li and Bhattacharya, 1989], and a monolithically integrated phototransceiver in which it was integrated with an LED [Qasaimeh, *et al.* 2000]. In the first case, the MBD and FET shared a common structure, and circuit utilized the MBD's gain and response speed. In the second case, the MBD's increasing gain with lower optical power was utilized to improve optical transceiver performance.

A symmetric gain optoelectronic mixer (SG-OEM) is being investigated for chirped-AM LADAR applications in this work. The device is based on a symmetric heterostructure, as shown in figure 1. The targeted operating wavelength is 1.55 μm. The emitter/collector is $In_{0.52}Al_{0.48}As$ (InAlAs), and the base is $In_{0.53}Ga_{0.47}As$ (InGaAs), both of which are lattice matched to the InP substrate. Through proper design, particularly of the $In_{0.52}Al_{0.48}As$ E/C layers, the device can have larger gain at lower optical power levels. Initial simulation studies at ARL used the one-dimensional SimWindows program. Two- and three- dimensional device simulations, using the Synopsis TCAD Sentaurus suite, are being carried out at the University of Maine to design optoelectronic mixers with suitable optical gain and frequency bandwidth. Two symmetric gain OEM heterostructures were grown at ARL using molecular beam epitaxy. Structure 1 has a base width of 800 nm and Structure 2 300 nm. Both Structures nominally have the same base doping of $2.5x10^{16}$ cm^{-3}. Prototype devices were fabricated at ARL, in collaboration with the University of Maine. Device diameters range from 18 μm to 30 μm. Preliminary I-V measurement data will be presented, and compared with the simulation predictions.

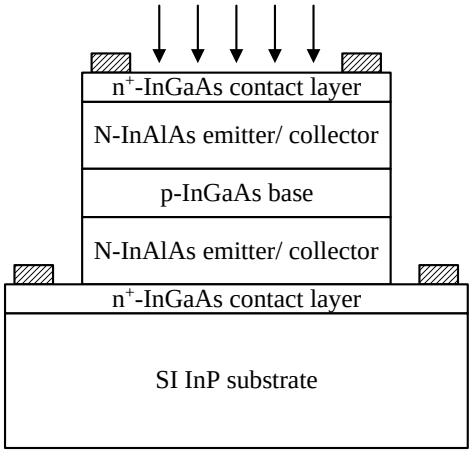

Fig. 1. Schematic structure of basic symmetric gain optoelectronic mixer.

2. SIMULATION STUDY AND DEVICE DESIGN

The initial one-dimensional device simulation study was done using SimWindows (copyright: David W. Winston). Both symmetric heterojunction phototransistors and symmetric modulated barrier diodes were investigated as candidates for the optoelectronic mixer. The effects of the layer thicknesses and doping densities were investigated for the two types of devices, including positional variation of the doping densities. The optimum for both types of devices converged to similar structures. The symmetric heterojunction phototransistor based structure was chosen for the symmetric gain optoelectronic mixer.

Two parameters need to be balanced in designing the SG-OEM. First, the responsivity needs to be highly symmetric, with as large a value as possible to make the device a practical alternative to the existing MSM-OEMs. Second, the device should turn on at low voltages, to avoid large power dissipation. These two requirements place contradictory constraints on the device design, resulting in a trade off between gain and turn-on voltage, and need to be optimized for specific applications.

The SG-OEM can be designed with a very symmetric responsivity, and the "turn on" voltage can be reduced to below 0.1 V, significantly reducing the voltage swing range for the device. The symmetric OEM behaves similar to a modulated barrier diode, in that the gain increases with decreasing optical power. This behavior is shown in figure 2, which presents the simulated DC responsivity curves of a sample device for incident optical powers ranging from 1 $\mu W/cm^2$ to 1 mW/cm^2. The device has a base thickness of 0.2 μm and doping of 10^{17} cm^{-3}, while the InAlAs layer doping is $4x10^{16}$ cm^{-3}.

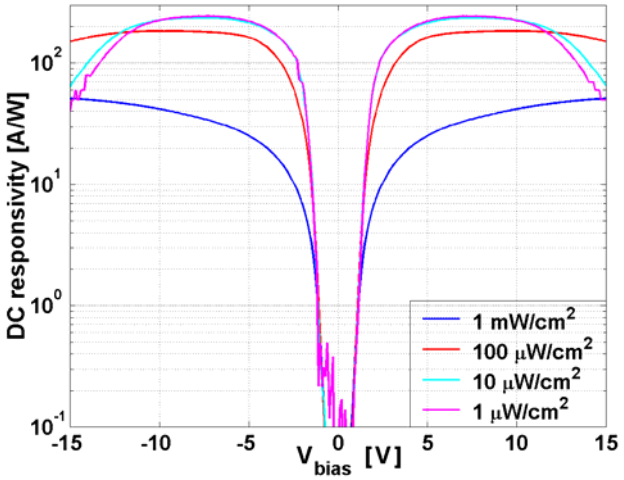

Fig. 2. DC responsivity of a sample OEM device, simulated with SimWindows.

Figure 3 presents the calculated mixing efficiency of this device as a function of the local oscillator (LO) voltage, for the same optical power levels as figure 2. As the LO signal is a radio frequency signal, the magnitude is given in dBm. The device would reach theoretical equivalence to the present InGaAs MSMs (~ 0.2 A/W mixing responsivity) [Shen, *et al.* 2003] at LO voltage levels of 11-12 dBm. An order of magnitude improvement would be achieved for 15-16 dBm (1.6 - 2 V peak), and two orders of magnitude improvement would be obtained at LO voltage levels of 23-25 dBm (4.5 – 5.6 V peak).

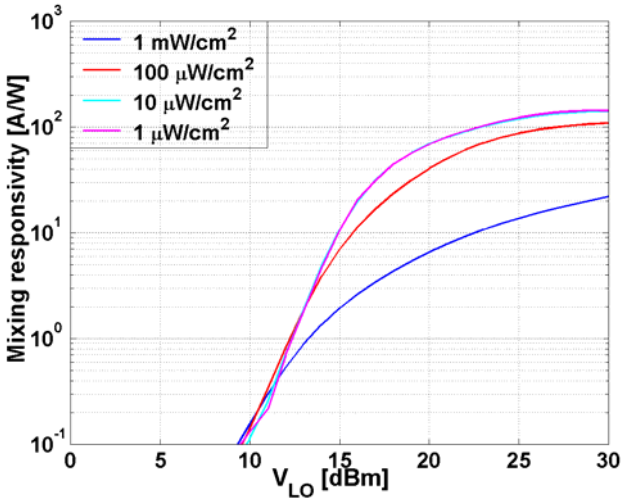

Fig. 3. Predicted mixing responsivity vs. LO voltage for the device of figure 2.

Two structures were selected for growth following the initial 1D simulation study. The layer structures of the two samples, Structure 1 and Structure 2, are shown in figure 4. Structure 1, with an 800 nm thick base layer, was chosen to ensure large photon absorption in the base layer, as absorption is proportional to the InGaAs layer thickness. Structure 2, with a 300 nm thick base layer, was chosen to maximize transistor gain, β, which is inversely proportional to base thickness.

A second important consideration was the contact layer. In traditional heterojunction bipolar junction transistors, a highly doped InGaAs layer is used as the contact layer for the InAlAs emitter. Better ohmic behavior is obtained if the metal contact is on the narrow bandgap InGaAs layer. Such an arrangement was used in Structure 1. In order to ensure that the active region etch stops in the bottom contact layer, this layer thickness was chosen to be 300 nm. Photon absorption in the heavily doped InGaAs layers is a concern, as this component of the photocurrent will not be amplified by the transistor action. Therefore, the InGaAs contact layer was eliminated for Structure 2, with a trade-off in increased ohmic contact resistance.

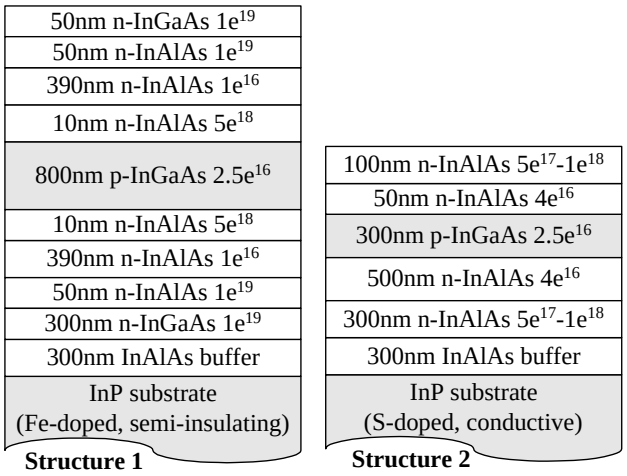

Fig. 4. Vertical structure of the two Structures selected for material growth and device fabrication.

Table 1. Simulated device parameters

	Size [μm]
Inner mesa	16
Outer mesa (bottom contact)	30
Top contact width	12
Top contact metal width	14
Bottom contact width	2
Bottom contact metal width	4
Bond pads	80 x 80

Detailed two-dimensional simulations were carried out to evaluate candidate device designs using the Synopsys® TCAD Sentaurus software suite. The Sentaurus Structure editor was used to construct the 2D device, and the simulations were performed using Sentaurus Device. Simulated I-V curves are presented below for the bottom-illumination device design summarized in Table 1.

Figure 5 shows the simulated current density profile in two dimensional cross section of a device on Structure 1, for a bias voltage of 10V applied to the top contact. The insulation layers and metal stack are not shown for clarity. The active area diameter is 16 μm, and the top contact diameter is 12 μm. The bottom contact is 2 μm wide. The distance between the bottom contact layer and the active region introduces a series resistance, which is apparent in the higher current density in this region. This series resistance results in a deviation from the 1D simulations, as will be discussed below. It also imposes a constraint on device fabrication, in that the penetration of the active region etch into the contact layer should be limited.

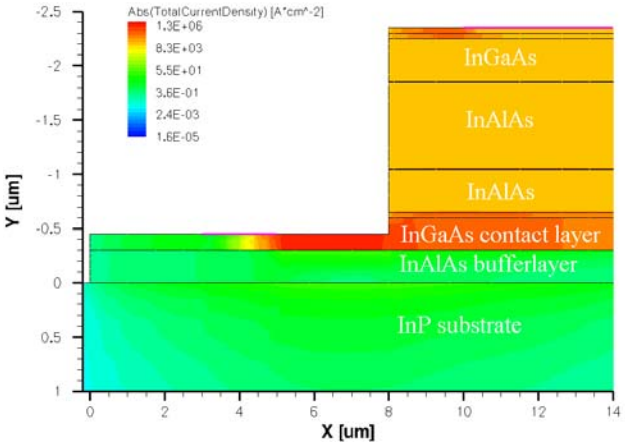

Fig. 5. Current density distribution in a device with the Structure 1 layer structure.

Figures 6 and 7 compare the forward and reverse bias currents for devices on Structure 1 and 2, with the dimensions listed in Table 1. There is a slight asymmetry in the I-V curves due to the asymmetry of the two structures. This asymmetry is more pronounced in Structure 2, due to the thicker bottom InAlAs layer.

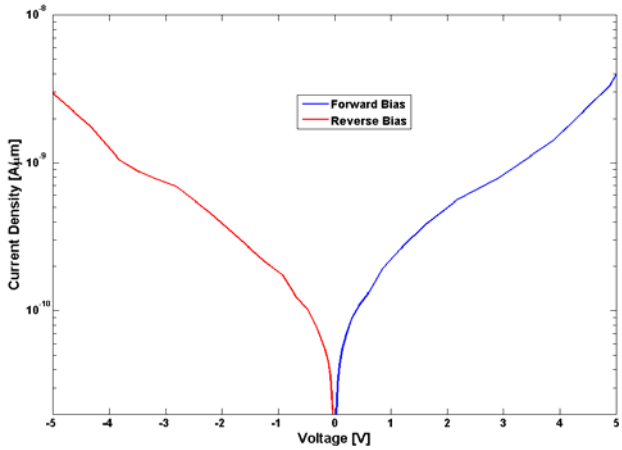

Fig. 6. Simulated I-V characteristics of an SG-OEM device on Structure 1, using TCAD-Sentaurus.

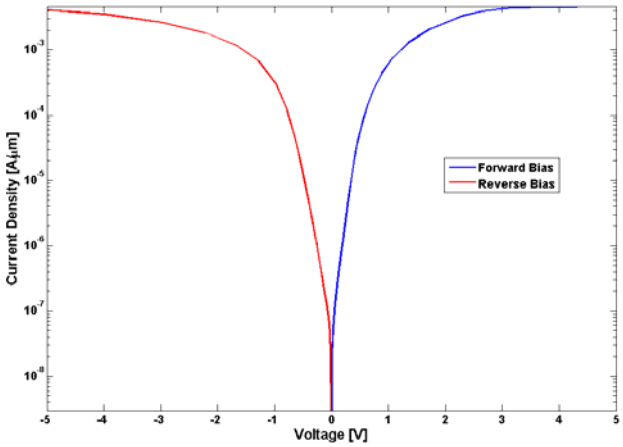

Fig. 7. Simulated I-V characteristics of an SG-OEM device on Structure 2, using TCAD-Sentaurus.

It should be noted that the 2D simulations predict different I-V characteristics for the devices in comparison with the original 1D simulations. This is due to the series contact resistance between the bottom contact and the active region of the device. Figure 8 compares the results of a 2D simulation with the 1D simulation for a device on Structure 2.

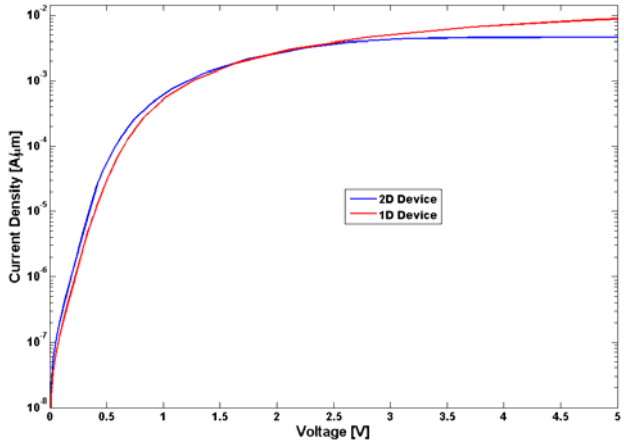

Fig. 8. Comparison of I-V characteristics for a SG-OEM device simulated in 1D and 2D, showing the effect of the bottom contact placements on SG-OEM performance.

3. MATERIAL GROWTH AND DEVICE FABRICATION

Mask design was done using Tanner L-Edit Pro 11. The die area is 1mm x 1mm. Each die has 32 devices of six basic designs, including square and circular devices. There are two types of circular devices, with ring contacts for top illumination and with circular contacts for bottom illumination through the substrate. The active area ranges from 18 μm to 30 μm for the circular devices, and from 10 μm to 16 μm for the square devices.

The two Structures were grown at ARL using molecular beam epitaxy. The two mesa etches (top contact and device isolation) were done with an RIE-ICP etcher, using a Cl_2/BCl_3 gas mixture. A 190 nm Si_3N_4 anti-reflection coating was deposited for the top-illumination devices. This layer also served as an insulation layer for the bond pads. An ohmic contact metallization scheme of 50Å Ni / 400Å Ge / 1500Å Au was used, annealed to 300°C in an N_2 ambient. Figure 9 shows a sample fabricated device, with a ring contact for top illumination.

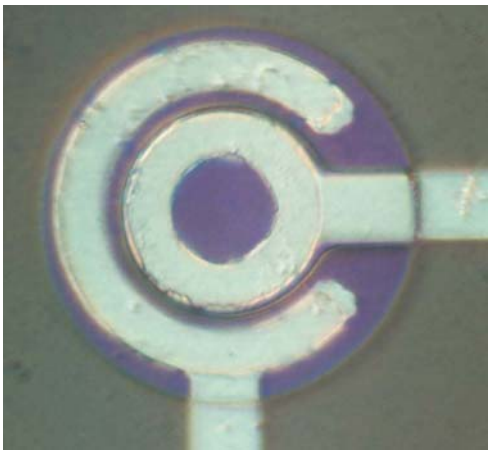

Fig. 9. Top-view photograph of a prototype symmetric gain optoelectronic mixer.

4. EXPERIMENTAL RESULTS

Current-voltage curves for two devices on Structure 2 with r = 9 μm are shown in figure 10. 'Dark' refers to the dark current of the devices, while 'light' refers to the microscope light on the probe station being turned on during measurement. The voltage was applied to the top contact, and the bottom contact was grounded. There is a slight asymmetry in the I-V curves, more visible in the reverse bias dark current, due to the asymmetry in the structure of Structure 2 (figure 4).

The measured currents for the first batch of the SG-OEM devices on structure 2 are about an order of magnitude smaller than predicted by simulation. We hypothesize that this is due to a large ohmic contact resistance between the metal – InAlAs contact layer. Contact resistance measurements will be carried out to determine the cause of this discrepancy.

Complete characterization of the prototype devices is in progress and will be presented in a subsequent article. The full characterization will include DC responsivity, frequency response (AC responsivity) and mixing efficiency (mixing responsivity).

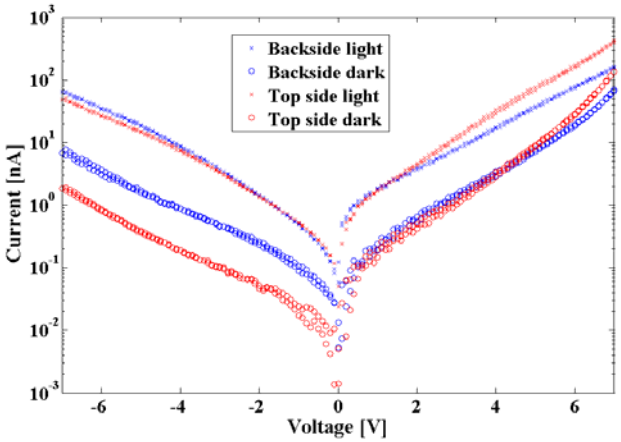

Fig. 10. I-V curves for top- (red) and back-side (blue) illumination devices with r = 9 μm.

CONCLUSIONS

Symmetric gain optoelectronic mixers are promising for chirped-AM LADAR systems developed at ARL. An optoelectronic mixer with gain allows a reduction of the following transimpedance amplifier's gain, increasing bandwidth and improving the system's noise performance. A simulation study identified structures based on symmetric heterojunction bipolar transistors as the most promising candidates for SG-OEM devices. Device designs were evaluated using 2D simulations. Two sample structures were grown by MBE. Prototype devices were fabricated. Preliminary I-V measurements are promising. Complete characterization of the prototype devices is in progress. These symmetric gain optoelectronic mixer devices can lead to miniaturized LADAR-on-chip system. Such a system will have many military and civilian applications, such as range finding, terrain mapping, reconnaissance, and face recognition.

ACKNOWLEDGEMENTS

We acknowledge Dr. Paul H. Shen and Dr. Wayne Chang for discussions regarding device design and development, and Dr. Stefan Svenson for growing the heterostructure samples. This research was partially funded by the US Army Research Office/ Laboratory through a Scientific and Technical Services Agreement issued by Battelle Chapel Hill Operations, TCN 07-058 under contract W911NF-07-D-0001.

REFERENCES

W. Ruff, J. Bruno, S. Kennerly, K. Ritter, P. Shen, B. Stann, M. Stead, G. Sztankay, M. Tobin, "Self-mixing detector candidates for an FM/cw ladar architecture", *Laser Radar Technology and*

Applications V, Proc. SPIE vol. 4035 p. 152-62, (2000)

H. Shen, K. Aliberti, "Theoretical analysis of an anisotropic metal-semiconductor-metal opto-electronic mixer", *J. Appl. Phys.*, vol. 91, no. 6, pp. 3880-90 (2002)

H. Shen, K. Aliberti, B. Stann, P. Newman, R. Mehandru, F. Ren, "Mixing characteristics of InGaAs metal-semiconductor-metal photodetectors with Schottky enhancement layers", *Appl. Phys. Lett.*, vol. 82, no. 22, pp. 3814-6 (June 2003)

H. Shen, K. Aliberti, B. Stann, P.G. Newman, R. Mehandru, F. Ren, "Analysis of InGaAs metal-semiconductor-metal OE mixers", *Physics and Simulation of Optoelectronic Devices XII, Proc. SPIE* vol. 5349, 197-205 (2004)

S. Chandrasekhar, M.K. Hoppe, A.G. Dentai, C.H. Joyner, G.J. Qua, "Demonstration of enhanced performance of an InP/InGaAs heterojunction phototransistor with a base terminal", *IEEE Elec. Dev. Lett.*, vol. 12, no. 12, pp. 550-552 (Oct. 1991)

F. Capasso, W.T. Tsang, C.G. Bethea, A.L. Hutchinson, B.F. Levine, "New graded band-gap picosecond phototransistor", *Appl. Phys. Lett.*, vol. 42, no. 1, pp. 93-95 (Jan. 1983)

J. Thuret, C. Gonzalez, J.L. Benchimol, M. Riet, P. Berdaguer, "High-speed InP/InGaAs heterojunction phototransistor for millimeter-wave fibre radio communications", *Proc. 11th Int. Conference on Indium Phosphide and Related Materials*, pp. 389-392 (1999)

C.S. Choi, J.H. Seo, W.Y. Choi, H. Kamitsuna, M. Ida, K. Kurishima, "60-GHz Bidirectional Radio-on-Fiber Links Based on InP–InGaAs HPT Optoelectronic Mixers", IEEE *Photon. Tech. Lett.*, vol. 17, no. 12, pp. 2721-3 (Dec. 2005)

J.L. Polleux, L. Paszkiewicz, A.L. Billabert, J. Salset, C. Rumelhard, "Optimization of InP–InGaAs HPT Gain: Design of an Opto-Microwave Monolithic Amplifier", *IEEE Trans. Microwave Theory Tech.*, vol. 52, no. 3, pp. 871-81 (Mar. 2004)

L.Y. Leu, J.T. Gardner, S.R. Forrest, "A high-gain high-bandwidth $In_{0.53}Ga_{0.47}As$/InP heterojunction phototransistor for optical communications", *J. Applied Physics*, vol. 69, no.2, p. 1052 (Jan. 1991)

C.P. Liu, A.J. Seeds, D. Wake, "Two-terminal edge-coupled InP/InGaAs heterojunction phototransistor optoelectronic mixer", *IEEE Microwave and Guided Wave Lett.*, vol. 7, no. 3, pp. 72-74 (March 1997)

J. Van de Casteele, J.P. Vilcot, J.P. Gouy, F. Mollot, D. Decoster, "Electro-optical mixing in an edge-coupled GaInAs/InP heterojunction phototransistor", *Elec. Lett.*, vol. 32, no. 11, pp. 1030-2 (May 1996)

C.Y. Chen, A.Y. Cho, P.A. Garbinski, C.G. Bethea, B.F. Levine, "Modulated barrier photodiode: A new majority-carrier photodetector", *Appl. Phys. Lett.*, vol. 39, no. 4, pp. 340-2, Aug. 1981

C.Y. Chen, "Theory of a modulated barrier photodiode", *Appl. Phys. Lett.*, vol. 39, no. 12, pp. 979-81, Dec. 1981

C.G. Bethea, C.Y. Chen A.Y. Cho, P.A. Garbinski, "Opto-electronic picosecond sampling system utilizing a modulated barrier photodiode", *Appl. Phys. Lett.*, vol. 40, no. 7, pp. 591-4, Apr. 1982

W.Q. Li, P.K. Bhattacharya, "Integration of a modulated barrier photodiode with a doped-channel quasi-MISFET", *IEEE Elec. Dev. Lett.*, vol. 10, no. 9, pp. 415-6, Sept. 1989

O. Qasaimeh, W.D. Zhou, P. Bhattacharya, D. Huffaker, D.G. Deppe, "Monolithically integrated low-power phototransceiver incorporating InGaAs/GaAs quantum-dot microcavity LED and modulated barrier photodiode", *Electronics Lett.*, vol. 36, no. 23, pp. 1955-7, Nov. 2000